Recovery of critical metals from EV batteries via thermal treatment and leaching with sulphuric acid at ambient temperature

Citation for the original published paper (version of record):
Petranikova, M., Naharro, P., Vieceli, N. et al (2022). Recovery of critical metals from EV batteries via thermal treatment and leaching with sulphuric
acid at ambient temperature. Waste Management, 140: 164-172.
http://dx.doi.org/10.1016/j.wasman.2021.11.030

Waste Management xxx (xxxx) xxx

Contents lists available at ScienceDirect

Waste Management

journal homepage: www.elsevier.com/locate/wasman

Recovery of critical metals from EV batteries via thermal treatment and leaching with sulphuric acid at ambient temperature

Martina Petranikova *, Pol Llorach Naharro, Nathália Vieceli, Gabriele Lombardo, Burçak Ebin

Chalmers University of Technology, Department of Chemistry and Chemical Engineering. Nuclear Chemistry and Industrial Materials Recycling, Gothenburg SE-412 96, Sweden

ARTICLE INFO

Keywords:
Li-ion batteries
Incinceration
Pyrolysis
Leachability
Ambient temperature
Process optimization

ABSTRACT

In the upcoming years, todaýs e-mobility will challenge the capacity of sustainable recycling. Due to the presence of organic components (electrolyte, separator, casings, etc.), future recycling technologies will combine thermal pre-treatment followed by hydrometallurgical processing. Despite the ongoing application of such treatment, there is still a lack of information on how applied parameters affect subsequent metal recovery. In this study, both oxidative and reductive conditions in dependence on temperature and time were studied. Qualitative and quantitative characterizations of the samples after treatment were performed followed by leaching with 2 M sulphuric acid at ambient temperature to determine the leachability of valuable metals such as Co, Mn, Ni and Li. Moreover, the negative or positive effect of treatment on the leachability of the main impurities (Cu and Al) was determined. Since the presence of carbon affects the degree of active material reduction, it's content after each thermal treatment was determined as well. If all variables, temperature and time of thermal processing are taken into account, pyrolysis at 700 °C for 30 min is the optimal treatment. Under these conditions, full recovery is reached after 2 min for Li, 5 min for Mn and 10 min for both Co and Ni. In the case of the incineration, only processing at 400 and 500 °C promoted higher recovery of metals, while the treatment at 600 and 700 °C led to the formation of less leachable species.

1. Introduction

Modern processing of spent lithium-ion batteries (LiBs) applies combined methods to achieve higher material recovery. At the same time, such an approach allows fulfilling regulations and rates required for example by the European Unioń directive. Thermal pre-treatment is mainly used to remove organic compounds and carbon that can interfere with posterior processing (Lombardo et al., 2020). This approach is already applied by several companies, such as Accurec (Germany), Redux (Germany), Fecupral (Slovakia), etc. In general, there are two types of thermal pre-treatment currently used in the industry: incineration (in the presence of oxygen) and pyrolysis (in the absence of oxygen). Also, vacuum pyrolysis has been applied to decompose $LiCoO_2$ and to separate lithium and cobalt (Huang et al., 2019; Sun and Qiu, 2011; Tang et al., 2019; Zhang et al., 2019). Some studies have been performed using the leaching process to determine the advantages (or disadvantages) of incineration and pyrolysis. Petranikova et al. (Petranikova et al., 2011) incinerated black mass at 300, 500 and 700 °C for 1 h to remove the organic compounds. It was proven that the cobalt leaching yield improved in the incinerated samples in comparison to untreated samples. Shin et al. (Shin et al., 2005) incinerated black mass at 900 °C. However, it was observed that cobalt leaching yield decreased in the incinerated samples in comparison to untreated samples. Afterwards, it was concluded that molten aluminium covered black mass particles decreasing the leaching yield. The most frequently used inorganic acids for leaching are HCl, H_2SO_4 and HNO_3 (Peng et al., 2020). Hydrochloric acid performs the best among these acids (Ordoñez et al., 2016). Zhang et al. (Zhang et al., 1998) reported that a leaching yield of more than 99% of cobalt and lithium could be achieved when 4 M HCl solution was used at a temperature of 80 °C and a reaction time of 1 h. Nan et al. (Nan et al., 2005) performed leaching with sulfuric acid. At higher acid concentration and reaction temperature, the leaching yield of cobalt was favoured. To further increase the acid leaching yield, reductive agents such as hydrogen peroxide have been tested. The presence of some reducing agent like H_2O_2 requires a lower acid concentration in the leaching media to yield the same concentration of lithium and cobalt in the leaching liquor (Porvali et al., 2020). This is because of the reduction of Co^{3+} to Co^{2+}, which can be readily dissolved (Lee and Rhee, 2003).

* Corresponding author.
E-mail address: martina.petranikova@chalmers.se (M. Petranikova).

https://doi.org/10.1016/j.wasman.2021.11.030
Received 6 May 2021; Received in revised form 7 November 2021; Accepted 18 November 2021

Lee et al. (Lee and Rhee, 2003) proved that by reductive leaching with the addition of hydrogen peroxide, the leaching yield increased by 45% for cobalt and 10% for lithium, comparing with leaching without H_2O_2 in the same leaching media. Meshram et al. (Meshram et al., 2015) leached all metals from cathode active material of LiBs with 1 M H_2SO_4 at 70 °C during 240 min. The optimal concentration of acidic leaching media varies between 2 and 4 M and the optimal concentration of hydrogen peroxide varies from 1 to 6 vol%. Leaching temperatures around 60–80 °C and leaching time of 1 h are the optimal conditions for cobalt and lithium leaching (Chagnes and Swiatowska, 2015). The use of hydrogen peroxide is required for manganese leaching as well. Despite the reduction of cathode material after pyrolysis, Sun et al. (Sun and Qiu, 2011) suggested that hydrogen peroxide should be used to achieve sufficient leaching yield for cobalt. However, the application of hydrogen peroxide represents a significant cost in the industrial processing. On the other hand, thermal pre-treatment provides the reduction of the oxides and by the selection of proper conditions, leaching efficiencies can be maximized even without the need for hydrogen peroxide.

Many recycling companies still perform incineration instead of pyrolysis, however, studies comparing both techniques have been rarely reported in the literature. Moreover, the effect of such thermal treatments on the impurities (Cu and Al) is also barely reported, but their removal causes significant losses of valuable metals. Thus, if their presence in the leachate can be eliminated by proper thermal pretreatment, it brings remarkable simplification of the processing as well as environmental impact. In this context, the main goal of this manuscript was to compare incineration and pyrolysis as a pre-treatemnt for LiBs and demonstrate the major differences between both processes when it comes to metal recovery using hydrometallurgy. Also, in the present study, the leaching process was performed at ambient temperature. Thus, the effect of the thermal treatment can be more precisely defined.

2. Materials and methods

Discharged pouch batteries were supplied by Volvo Car Corporation. The chemistry of the battery cells was identified as a mixture of $LiCoO_2$, $LiMn_2O_4$ and $LiNiO_2$. Pouch batteries were cut to smaller pieces using a puncher. Subsequently, grinding with an IKA M20 universal mill crusher was applied for one hour to obtain homogenous samples. The final particle size was under 75 μm.

2.1. Thermal pre-treatment

Samples after crushing and homogenization were inserted in a quartz tube (700x30 mm). The weight of the sample was 6 g for each experiment. A tubular furnace, Nabertherm GmbH Universal Tube Furnace RT 50–250/11 – RT 30–200/15 (Lombardo, 2019), was used to perform the thermal treatment of the samples. A constant flow of 340 mL/min of N_2 (99.9%) was used when pyrolysis was performed. In the incineration process, a constant air flow rate of 340 mL/min was sustained. The samples were heated at 400, 500, 600 and 700 °C. The sample was inserted in the tube to the center of the furnace and kept there for 30, 60 or 90 min. The loss in sample weight was examined by weighing the samples before and after the experiment. Experiments were carried out in triplicate.

2.2. Leaching

For the leachability study, samples (before and after thermal treatment) were leached with 2 M sulfuric acid for 180 min and solid to liquid ratio 1:50 (g/mL), to minimize the effect of sampling. The weight of the sample was 0.5 g and volume of the acid was 25 mL. Agitation was accomplished by magnetic stirring at 300 rpm. Experiments were performed in triplicates. Once the sample was introduced in the acid solution previously heated at the required temperature, the agitation started. In order to study the yield of the leaching reaction, samples were taken every 1, 2, 5, 10, 15, 45, 60, 90, 120 and 180 min. The volume of the sample for the analysis was 100 μL, to minimize the effect of sampling. The leaching liquor was filtered using a vacuum system (Lafil 400-LF30/ SMI-LabHut Ltd). The dry solid residue was weighted to determine the weight loss during the leaching in comparison with the mass of the initial sample for a more precise determination of mass balance. The leaching yield was calculated using the following equation,

$$\eta_i = \frac{C_i V}{m_0 \omega i} \times 100(A)$$

where,

C_i (ppm or mgL^{-1}) - concentration of metal ion 'i' in the solution, V (L) - volume of leaching solution, m_0 (mg) - mass of pretreated material, ω_i - weight content of the element i in the sample.

2.3. Samples analysis

Qualitative analysis was performed using X-ray diffraction analysis by Siemens D5000 X-ray diffractometer, with an accelerator voltage of 40 kV and a current of 40 mA. The X-ray wavelength used corresponds to the characteristic Cu K-radiation and a 2Θ range from 10° to 80° was included in the scans. Sample rotation was set at 15 rpm to avoid the effect of any preferential orientation of the crystals giving rise to incorrect peak heights. Analytical interpretation was performed using EVA software and a Powder Diffraction File (PDF®) database from ICDD (International Center for Diffraction Data). The total content of metals in the solid samples was determined after the digestion of samples (0.2 g) in aqua regia (50 mL), at 80 °C under magnetic stirring during 360 min. Three sample replicates were investigated to account for heterogeneity. After the digestion, the liquid samples were diluted with 0.5 M nitric acid solution, and the metal content was determined using Inductively Coupled Plasma-Optical Emission Spectroscopy (ICP-OES) (iCAP 6500. Thermo Fisher) and Inductively Coupled Plasma- Mass Spectroscopy (ICP-MS) (iCAP Q. Thermo Fisher). The same analytical method was used to determine the metal content in the samples after leaching. Thermodynamic data related to the leaching process were calculated using HSC Chemistry 9 software (Outotec, 2016).

3. Results and discussion

3.1. Material characterization

The metal composition of the samples varies after each different thermal treatment due to the carbothermic reduction and electrolyte decomposition. The total weight of the samples was reduced, and metals were pre-concentrated. Since carbon elimination is enhanced at higher temperatures, as expected, the decrease in the carbon content in the samples is proportional to the increase in temperature. Table 1 shows the composition of every sample after the incineration and pyrolysis at 400 °C, 500 °C, 600 °C and 700 °C during 30, 60 and 90 min. Data for the untreated sample is also included.The heterogeneous character of the samples was taken into consideration. It was concluded that except untreated samples, treated samples do not exhibit any significant trend related to the metal content, despite the long reaction time.

3.2. Thermodynamic considerations for leaching process

The mechanism of expected reactions is shown in Table 2. Thermodynamic data for $LiNiO_2$ are not included in HSC Chemistry database and thus this cathode material was excluded from the following section. The modelling showed that with increasing temperature the change of Gibbs free energy reaches more negative values for the majority of the reactions and therefore are more likely to occur spontaneously. Reactions in bold exhibit positive values of ΔG^0.

Table 1
Weight percentage of major metals and carbon present in untreated samples (UT) and samples incinerated (I) and pyrolyzed (P) at different temperature and time.

T(°C)	Time[min]		Mn	Ni	Co	Cu	Li	Al	C
		UT	11.0 ± 0.7	5.6 ± 0.3	5.5 ± 0.3	12.3 ± 0.8	2.4 ± 0.2	6.8 ± 0.5	40.8 ± 2.8
400	30	I	12.2 ± 0.1	6.2 ± 0.1	6.1 ± 0.1	14.2 ± 0.1	2.6 ± 0.1	7.0 ± 0.1	29.6 ± 1.4
		P	11.4 ± 0.3	6.0 ± 0.3	5.7 ± 0.3	12.9 ± 0.1	2.6 ± 0.3	7.1 ± 0.3	35.5 ± 2.4
	60	I	12.8 ± 0.2	6.3 ± 0.2	6.5 ± 0.1	15.4 ± 0.1	2.6 ± 0.1	7.9 ± 0.2	25.0 ± 1.5
		P	11.6 ± 0.2	6.2 ± 0.3	5.8 ± 0.1	13.1 ± 0.2	2.6 ± 0.1	7.3 ± 0.1	32.8 ± 2.0
	90	I	13.2 ± 0.2	6.5 ± 0.2	6.4 ± 0.2	15.6 ± 0.5	2.7 ± 0.1	7.7 ± 0.4	19.1 ± 2.3
		P	11.8 ± 0.2	6.3 ± 0.3	5.9 ± 0.3	13.4 ± 0.3	2.7 ± 0.3	7.4 ± 0.3	21.2 ± 1.6
500	30	I	12.9 ± 0.2	6.8 ± 0.1	6.2 ± 0.4	15.6 ± 0.3	2.7 ± 0.1	7.9 ± 0.3	24.0 ± 2.2
		P	11.7 ± 0.3	5.9 ± 0.3	5.7 ± 0.3	13.0 ± 0.3	2.8 ± 0.2	6.0 ± 0.3	32.0 ± 2.5
	60	I	13.1 ± 0.2	6.9 ± 0.2	6.6 ± 0.3	15.9 ± 0.4	3.4 ± 0.1	8.1 ± 0.5	21.5 ± 1.2
		P	12.8 ± 0.5	6.1 ± 0.3	6.3 ± 0.3	13.4 ± 0.2	2.8 ± 0.3	7.1 ± 0.2	31.7 ± 2.5
	90	I	14.3 ± 0.2	6.9 ± 0.1	6.8 ± 0.1	16.9 ± 0.3	3.6 ± 0.1	8.7 ± 0.2	15.7 ± 1.2
		P	13.2 ± 0.3	6.7 ± 0.3	6.6 ± 0.3	15.3 ± 0.1	3.1 ± 0.3	7.5 ± 0.3	23.3 ± 1.2
600	30	I	13.4 ± 0.2	6.8 ± 0.2	6.3 ± 0.1	15.3 ± 0.5	2.6 ± 0.1	7.4 ± 0.1	16.0 ± 1.3
		P	11.7 ± 0.2	6.2 ± 0.3	5.7 ± 0.3	12.5 ± 0.1	2.7 ± 0.2	7.4 ± 0.3	31.4 ± 1.7
	60	I	13.8 ± 0.3	7.6 ± 0.1	6.6 ± 0.5	16.6 ± 0.3	2.8 ± 0.1	8.0 ± 0.4	11.9 ± 1.0
		P	12.6 ± 0.1	6.3 ± 0.1	6.1 ± 0.1	13.6 ± 0.2	2.4 ± 0.3	7.3 ± 0.3	29.4 ± 2.5
	90	I	14.2 ± 0.3	7.5 ± 0.2	7.3 ± 0.1	16.9 ± 0.1	3.8 ± 0.1	8.8 ± 0.1	5.5 ± 1.0
		P	13.2 ± 0.3	6.7 ± 0.3	6.6 ± 0.3	14.4 ± 0.3	3.1 ± 0.3	9.9 ± 0.3	21.1 ± 1.6
700	30	I	13.9 ± 0.2	6.9 ± 0.1	6.8 ± 0.1	16.3 ± 0.2	2.9 ± 0.1	8.7 ± 0.3	5.3 ± 0.9
		P	12.0 ± 0.1	6.5 ± 0.1	5.9 ± 0.1	13.6 ± 0.3	2.9 ± 0.1	8.2 ± 0.1	27.2 ± 2.5
	60	I	14.2 ± 0.3	7.4 ± 0.1	7.3 ± 0.3	16.5 ± 0.1	2.9 ± 0.1	9.7 ± 0.5	2.2 ± 0.2
		P	12.2 ± 0.1	7.0 ± 0.3	6.2 ± 0.3	14.3 ± 0.1	3.0 ± 0.3	10.1 ± 0.1	25.2 ± 0.6
	90	I	15.0 ± 0.4	7.7 ± 0.1	7.6 ± 0.1	17.0 ± 0.5	3.2 ± 0.1	9.8 ± 0.3	0.6 ± 0.2
		P	14.2 ± 0.3	7.1 ± 0.2	6.7 ± 0.3	15.1 ± 0.3	3.0 ± 0.3	10.3 ± 0.2	16.0 ± 1.6

Table 2
The change of Gibbs free energy of the reactions between active materials, by-products, impurities, and leaching media in dependence on the temperature.

		Reaction mechanism	ΔG^0_{25} [kJ/mol]	ΔG^0_{40} [kJ/mol]	ΔG^0_{60} [kJ/mol]
Co	(1)	$4LiCoO_2 + 6H_2SO_4 = 4CoSO_4 + 2Li_2SO_4 + O_2 + 6H_2O$	−595.6	−599.0	−601.6
	(2)	$2Co_3O_4 + 6H_2SO_4 = 6CoSO_4 + 6H_2O + O_2$	−372.6	−375.9	−379.4
	(3)	$CoO + H_2SO_4 = CoSO_4 + H_2O$	−115.5	−115.1	−114.6
	(4)	$Co + H_2SO_4 = CoSO_4 + H_2$	−92.2	−93.4	−94.6
Mn	(5)	$2LiMnO_4 + 3H_2SO_4 = Li_2SO_4 + 2MnSO_4 + 3H_2O + 2.5O_2$	− 283.7	−292.1	−302.0
	(6)	$2Mn_3O_4 + 6H_2SO_4 = 6MnSO_4 + 6H_2O + O_2$	−271.7	−278.3	−286.5
	(7)	$2Mn_2O_3 + 4H_2SO_4 = 4MnSO_4 + 4H_2O + O_2$	−130.5	−136.1	−142.9
	(8)	$MnO + H_2SO_4 = MnSO_4 + H_2O$	−110.5	−110.8	−111.4
	(9)	$MnO_2 + H_2SO_4 = MnSO_4 + H_2O + O_2$	−15. 5	−20.4	−26.0
Ni	**(10)**	**$2NiO + 2H_2SO_4 = 2NiSO_4 + 2H_2 + O_2$**	**279.7**	**274.2**	**268.7**
	(11)	$Ni + H_2SO_4 = NiSO_4 + H_2$	−72.2	−73.1	−73.9
Li	(12)	$Li_2O + H_2SO_4 = Li_2SO_4 + H_2O$	−262.4	−263.6	−265.1
	(13)	**$2LiF + H_2SO_4 = Li_2SO_4 + 2HF$**	**41.3**	**35.2**	**28.9**
	(14)	$Li_2CO_3 + H_2SO_4 = Li_2SO_4 + H_2O + CO_2$	−85.1	−89.5	−94.2
Cu	**(15)**	**$Cu + H_2SO_4 = CuSO_4 + H_2$**	**65.4**	**65.6**	**64.9**
	(16)	$CuO + H_2SO_4 = CuSO_4 + H_2O$	−44.6	−43.3	−42.3
	(17)	$Cu_2O + H_2SO_4 = CuSO_4 + Cu + H_2O$	−24.3	–22.6	−21.4
Al	(18)	$2Al + 3H_2SO_4 = Al_2(SO_4)_3 + 3H_2$	−1053	−1055	−1057
	(19)	$Al_2O_3 + 3H_2SO_4 = Al_2(SO_4)_3 + 3H_2O$	−103.1	−93.7	−85.5
	(20)	**$2AlF_3 + 3H_2SO_4 = Al_2(SO_4)_3 + 6HF$**	**213.6**	**230.7**	**247.6**

3.3. Leaching of untreated samples

To determine the effect of the thermal treatment on further metal recovery, samples without any pre-treatment were leached to obtain the reference parameters. Both leaching kinetics and leaching yield were improved when the temperature of the reaction increased. After 180 min of leaching in 2 M H_2SO_4, the leaching yield of Li improved from approximately 71%- 84% at 40 °C to 97% at 60 °C. The leaching yield of divalent metals was much lower than the yield of Li. The reason is the complex structure of cathode materials and metal ions incorporation, while Li is also present in the "free" electrolyte present in the untreated samples, whichcan be recovered directly. Additionally, transition metals present in LiBs generally require reductive conditions to form more easily leachable compounds. Thus, under the tested conditions without reducing agents, lower leaching yields were expected for transition metals when compare to Li. The maximum leaching yield was 76% for Mn, 85% for Ni and 88% for Co at 60 °C after 180 min of leaching with 2 M H_2SO_4. Since Cu needs oxidative conditions to be leached, the yield of its recovery was around 10% only. The leaching yield of Al was under 40% at 60 °C.

3.4. Leaching of incinerated samples

The leaching yield was assumed to increase with the treatment temperature due to removal of binder and hydrophobic organic components. In order to compare and obtain conclusions from the results, the leaching yield of incinerated samples was studied. The leaching time was 3 h at 25 °C was selected. Low leaching temperature was used to eliminate its effect on the leaching process and to fully observe the effect of thermal pre-treatment. The same leaching conditions were tested for untreated samples.

It follows from the results that the highest leaching yield of Co and Ni was achieved mostly for untreated samples, and samples incinerated at 400 °C and 500 °C. After that, a remarkable decrease of yield is reported, which is even lower than untreated samples. On the other hand, Li yield increases up to a maximum of 84% at 600 °C with a minor difference from the results at 500 °C (83%).

Fig. 1 exhibits the leaching yield of metals from incinerated samples. In these charts, the low values for incinerated samples at 700 °C can be clearly determined for all the metals. In order to determine the effect of

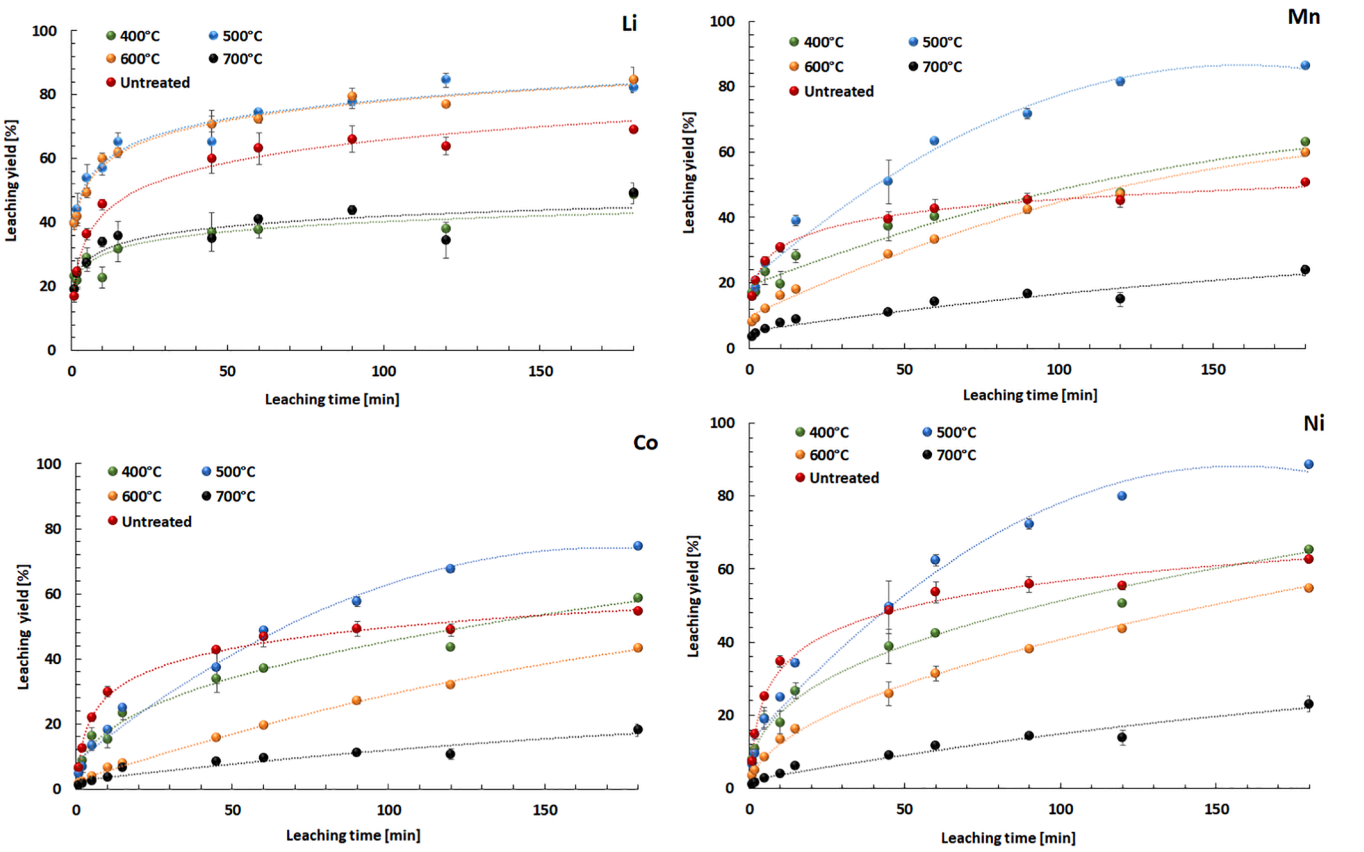

Fig. 1. Leaching yield of Li, Mn, Co and Ni from incinerated samples after 1 h of incineration. Leaching media: 2 M H_2SO_4 at 25 °C after 180 min. The sequence of the plots: Li; Mn; Co and Ni.

the incineration on the leachability, X-ray diffraction analyses (Fig. 2) was performed for the samples before and after leaching.

Fig. 2 shows the XRD patterns for incinerated samples for 1 h before leaching with H_2SO_4 and the XRD patterns for incinerated samples for 1 h after leaching and vacuum filtering of the leachate.

The peak at 18° confirms the presence of $LiNi_xCo_yMn_zO_2$ ($0 \leq x,y,z \leq 1$) and $LiNi_xCo_yMn_{2-x-y}O_4LiCoO_2$, $LiMn_2O_4$ ($0 \leq x,y \leq 1$). For samples before leaching, this peak remains constant with a slightly decrease when the incineration temperature increases. According to Lombardo (Lombardo, 2019) incineration at 700 °C for 1 h can remove almost all the organic compounds from the samples, making the carbothermic reduction of metal oxides more difficult. The peak at 26.5° is characteristic for graphite. The intensity of this peak decreases as well as the incineration temperature increases until it is finally inappreciable at 700 °C. The high intensity of the graphite peak for the incinerated sample at 400 °C can be possible due to the different distribution of carbon content from heterogeneous samples and to the lower removal of graphite at this temperatute (cf. Table 1) . This may explain the different proportion of graphite and, in addition, the low leaching yield for Li due to an excess of carbon in the samples associated to the use of room temperature in the acid leaching. Expected products from the carbothermic reduction of $LiCoO_2$, $LiMn_2O_4$ and $LiNiO_2$ can be spotted at 700 °C: $Co^{(3+)}$ present in $LiCoO_2$ is reduced to $Co^{(2+)}O$ and $Mn^{(3+)(4+)}$ present in $LiMn_2O_4$ is reduced to $Mn^{(3+)}{}_2O_3$ and MnO_2. Also, $Ni^{(3+)}$ present in $LiNiO_2$ is reduced to $Ni^{(2+)}O$. This change is responsible for a lower leachability of Ni and Mn from the sample incinerated at 700 °C. Processing at given temperature promotes the formation of NiO, which reaction with sulphuric acid exhibits positive change of Gibbs free energy (Equation 10). Despite slightly negative values of change of Gibbs free energy for the leaching of MnO_2 (Equation 9), it is known that MnO_2 is not soluble in sulphuric acid and reductive conditions have to be used (Toro et al., 2021). Lower leachability of Li (Fig. 1) can be explained by the formation of LiF, also identified in the sample solid residue after leaching (Fig. 2), which has positive values of change of Gibbs free energy (Equation 13). Moreover, other oxides are also formed from the Al and Cu current collectors since the O_2 in the gas flow causes their oxidation. The spectra for incinerated samples at 700 °C show the presence of Al_2O_3 and CuO. The most predominant species are graphite, Cu, Al and oxides of these two metals (Lombardo, 2019). However, in the spectra for the solid residues of incinerated samples at 700 °C and 600 °C, the peaks for $CoMn_2O_4$, $NiMn_2O_4$ and Co-Ni alloy were detected. Since those structures are very stable, lower leachability is a consequence of their formation at given conditions. The final carbon content in the samples after incineration is listed in Table 1.

The kinetic study shows that carbon is consumed for the carbothermic reduction and oxidized with the oxygen from the air throughout the whole tested process. The lowest concentration was detected after processing at 700 °C for 90 min. The main advantage of carbon removal, except its utilization for the carbothermic reduction, is the simplification of the solid to liquid separation after the leaching.

3.5. *Leaching of the impurities after incineration*

In general, Cu and Al are considered to be the main impurities for the hydrometallurgical processing of Li-ion batteries. Usually, those elements are removed before the separation of Mn/Ni/Co by solvent extraction (Mantuano et al., 2006). Due to that, it is necessary to define the positive or negative influence on their leaching achieved by the incineration. Fig. 3 exhibits the leaching yield of Cu and Al after the incineration at different temperature and time of the processing after 1 h of leaching

Due to the oxidation conditions, Cu oxidizes from $Cu^{(0)}$ to $Cu_2{}^{(1+)}O$ or $Cu^{(2+)}O$. Its leaching yield increased from 10% without the pretreatment to over 60% after the incineration at 500 °C. The highest

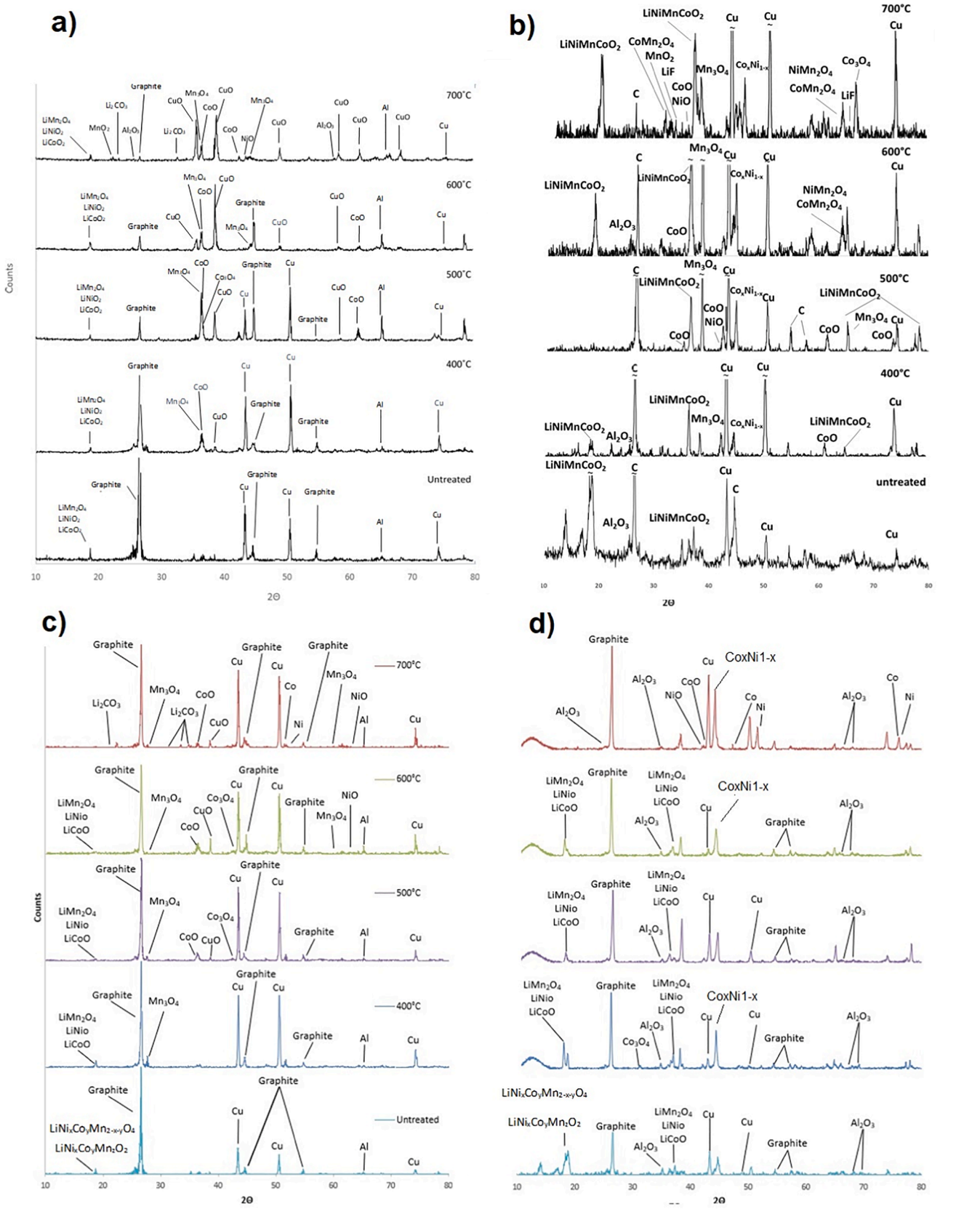

Fig. 2. XRD patterns of samples incinerated at different temperatures (a) and XRD of solid residues after leaching incinerated samples (b) and XRD patterns of samples pyrolysed at different temperatures (c) and XRD of solid residues after leaching incinerated samples (d).

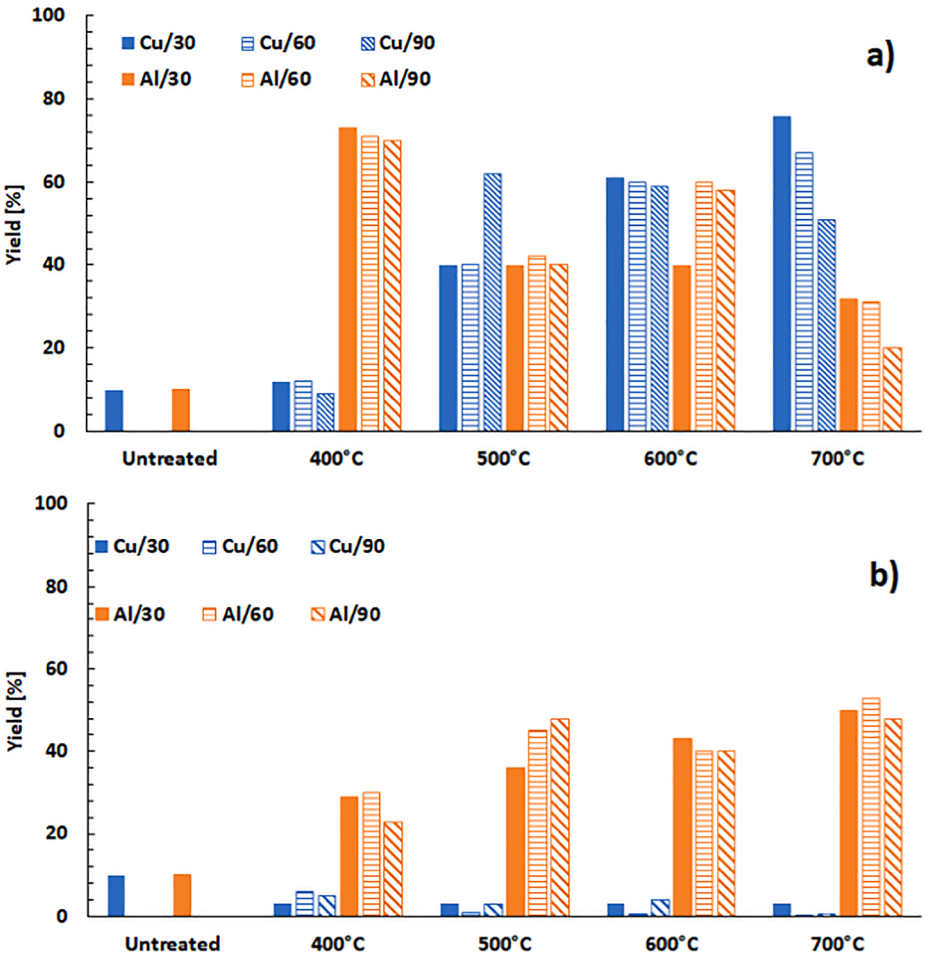

Fig. 3. Leaching yield of Cu (orange bars) and Al (blue bars) from the incinerated (a) and pyrolyzed (b) samples after different duration (30, 60 and 90 min) of the processing. Leaching conditions: 1 h, 25 °C, 2 M H_2SO_4, solid to liquid ratio of 1:50 (g/mL). (For interpretation of the references to colour in this figure legend, the reader is referred to the web version of this article.)

yield was achieved after treatment at 700 °C. The main reason for such performance is that Cu leaching requires oxidative conditions. According to the change of Gibbs free energy value for the reaction (15–17) in the Table 2, the reaction of Cu leaching has positive values of ΔG^0 and it not favourable from the thermodynamic point of view. On the other hand, leaching of CuO and Cu_2O is thermodynamically feasible. The leaching yield of Cu decreased after the treatment at 700 °C in the dependence of time. The change of Gibbs free energy for Cu oxidation reaches less negative values with increasing temperature. Also, Cu was detected by XRD analysis (Fig. 2) of the solid residue after the leaching, which confirms the reaction mechanism according to the reaction (17).

Incineration promoted Al leaching as well. Leaching yield increased from 10% (untreated sample) to over 70% after the incineration at 400 °C. Such development confirms the reaction mechanism according to the reaction (18), which show that Al leaching is thermodynamically favourable. At higher temperature the oxidation degree of Al increased, and leaching mechanism was performed according to the reaction (19), which represents leaching of Al_2O_3 due to the oxidation of the Al surface. Fluorination of Al can occur as well and AlF_3 can be formed after the reaction of Al with HF, which is the product of electrolyte decomposition (Balachandran et al., 2021). Also, thin film methods such as atomic layer deposition can be used to deposit thin layers (e.g., Al_2O_3 or AlF_3) onto cathode materials to protect them from side reactions with the electrolyte, such as transition metal dissolution. AlF_3 was not detected by the XRD analysis as its concentration was under the detection limit but its reaction with sulphuric acid was considered in the thermodynamic considerations as it is assumed to be present.

3.6. Leaching of pyrolyzed samples

Samples after pyrolysis follow a more consistent trend in terms of leaching yield in comparison with incinerated samples. It is clear that the leaching yield is enhanced when the temperature of pyrolysis increases. The following Fig. 4 shows the evolution of leaching yield. Pyrolysis temperatures of 400 °C, 500 °C, 600 °C and 700 °C are compared with the yield of untreated samples.

The leaching yield of all metals increased already in the samples pyrolyzed at 400 °C. The main reason of such improvement is the start of the decomposition of polymers, such as the binder (PVDF) and separator, which occurs around 400 °C. This allows for better access of the leaching media to the active material and helps to partially decompose the active material as it can be seen on the XRD data of pyrolyzed samples (Fig. 2). Pyrolysis at 400 °C improved leaching yield by 20%. Samples treated at 500 °C and 600 °C also exhibit better leaching yield. Significant improvement was achieved for the samples treated at 700 °C. Kinetics of the reaction increased and the maximum yield of Li and Mn was reached in<5 min for the sample pyrolyzed at 700 °C. The maximum Co and Ni yields were reached after 2 h of leaching.

Similar results are obtained when pyrolysis time was increased. The dependence of Li and Mn yields on the pyrolysiśs time is shown in Fig. 5 (top). Co and Ni yields after the same treatment are shown in Fig. 5 (bottom). Values are given after 1 h of leaching with 2 M H_2SO_4 at ambient temperature. The most efficient treatment temperature was still 700 °C and yield from untreated samples was the least efficient and slowest in terms of kinetic behaviour. However, longer treatment time at

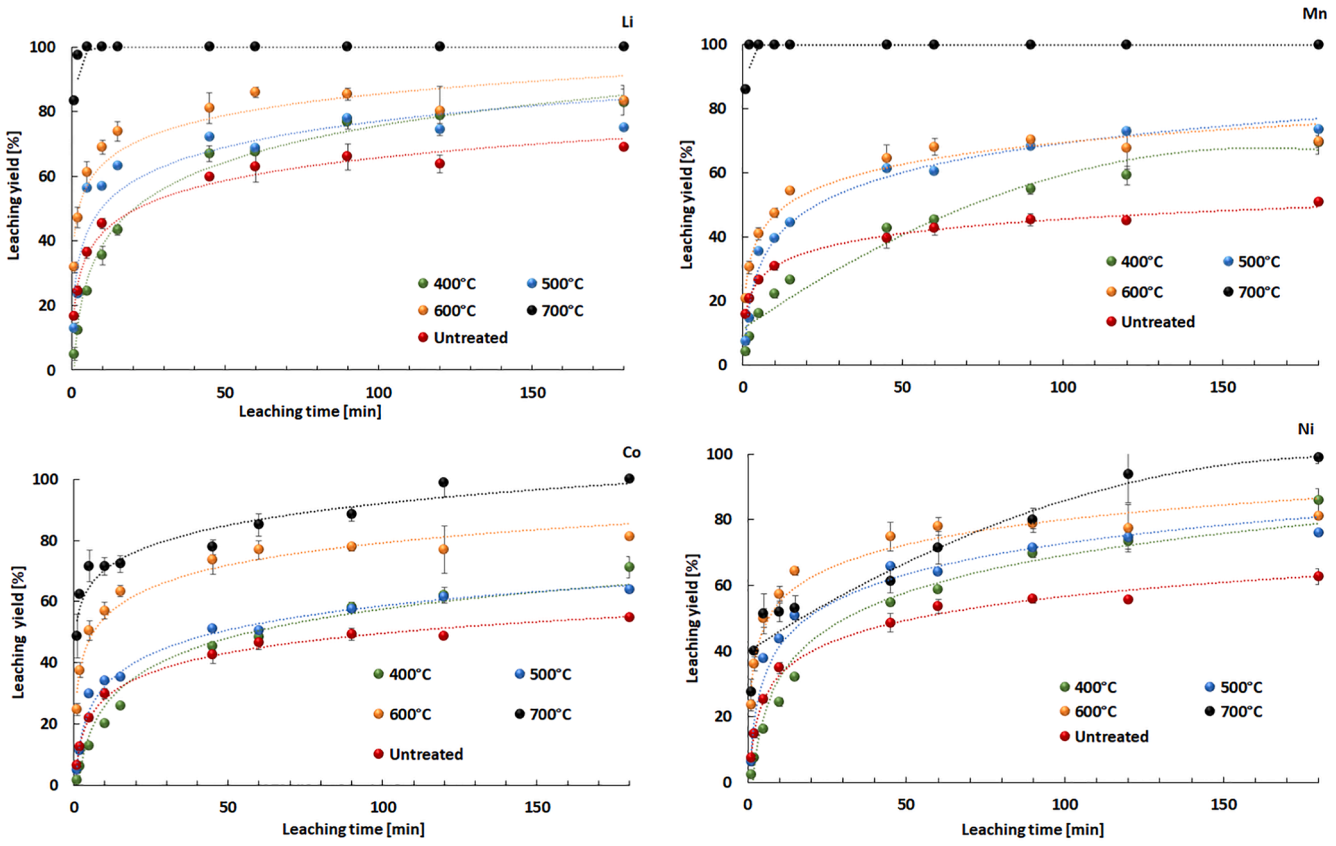

Fig. 4. Leaching yield of Li, Mn, Co and Ni from samples after 1 h of pyrolysis. Leaching media: 2 M H_2SO_4 at 25 °C after 180 min. Sequence of the plots: Li; Mn; Co and Ni.

700 °C leads to the decreasing trend in Co and Ni recovery. The main reason is the formation of more complex structures after long time of the treatment or formation of less leachable metal oxides such as $CoMn_2O_4$ or $NiMn_2O_4$.

XRD patterns of pyrolyzed samples are shown in Fig. 2. It is confirmed that the active materials were reduced almost completely after treatment at 600 and 700 °C to Co, Ni and Mn oxides or their metallic forms. Since the presence of oxygen was limited, residual graphite is present after the treatment at each temperature. Other present species are Cu and Al. After the leaching, all solid residues were analysed using XRD. Major phases were C, Cu and Al_2O_3. Despite high leaching efficiencies, Ni and Co oxides and their metallic forms were still detected, however the residual content might be a consequence of high consumption of the acid due to metal pre-concentration after pyrolysis.

3.7. Leaching of the impurities after pyrolysis

Similarly to the incineration, the leaching of the impurities has been compared in the dependence on the temperature and time of the treatment (Fig. 3). Since reductive atmosphere inhibits Cu oxidation, Cu leaching yield was very low. Cu was present in the samples as $Cu^{(0)}$. As mentioned before, Cu leaching requires oxidative conditions. While Cu yields is approximately 10% from the untreated samples, yield of Cu from pyrolyzed samples varies from 1% after treatment at 700 °C to approximately 6% after pyrolysis at 400 °C. This confirms that the reaction mechanism was performed according to the reaction (15), which represents Cu leaching. It can be concluded that by selection of the pyrolysis as a pre-treatment tool, Cu presence in the leachate can be eliminated. This will improve further hydrometallurgical processing since Cu removal will not be necessary.

Comparably to Cu, Al oxidation was inhibited during the pyrolysis as well. However according to the reaction (18) and (19), leaching of Al in the form of $Al^{(0)}$ is more favourable than leaching of Al_2O_3 – from the thermodynamic point of view. Leaching yield of Al increased from 10% from the untreated samples to approximately 50% after pyrolysis at 700 °C.

Since pyrolysis was performed at the limited presence of oxygen, the carbon content in the pyrolyzed samples was much higher than in the samples after the incineration. Residual carbon content is shown in Table 1.

3.8. Comparison between incineration and pyrolysis

There is a significant difference in the kinetics of incinerated and pyrolyzed samples. Kinetic of the leaching is faster for pyrolyzed samples. Moreover, results for pyrolyzed samples are more consistent and always follow the same trend: leaching yield and kinetics are enhanced by the rise of the thermal treatment temperature, with the exception of 700 °C where the molten aluminium has an impact on metal leachability. Table 3 ranks the treatment temperature for incinerated samples in ascending order of leaching kinetics for Li, Mn, Co and Ni.

During the incineration process, the oxygen flow introduced oxidises the carbon present in the samples to CO_2 instead of CO, thus the carbon present has a limited effect on the reduction of the metal oxides. Therefore, a partial carbothermic reduction can occur during the incineration process given the access of carbon, despite the presence of the oxygen from the air. In that case, a reduction media – CO(g) is formed as the by-product of the carbon oxidation. CO(g) reacts with metal oxides and leads to their reduction. However, the presence of oxygen mainly causes the oxidation of metallic foils, such as Cu and Al. This effect does not apply for the pyrolysis process, performed in an inert nitrogen-rich atmosphere, where carbothermic reduction of metal oxides is achieved in a more consistent and controlled way.

To summarize, pyrolysis is a better thermal treatment method than

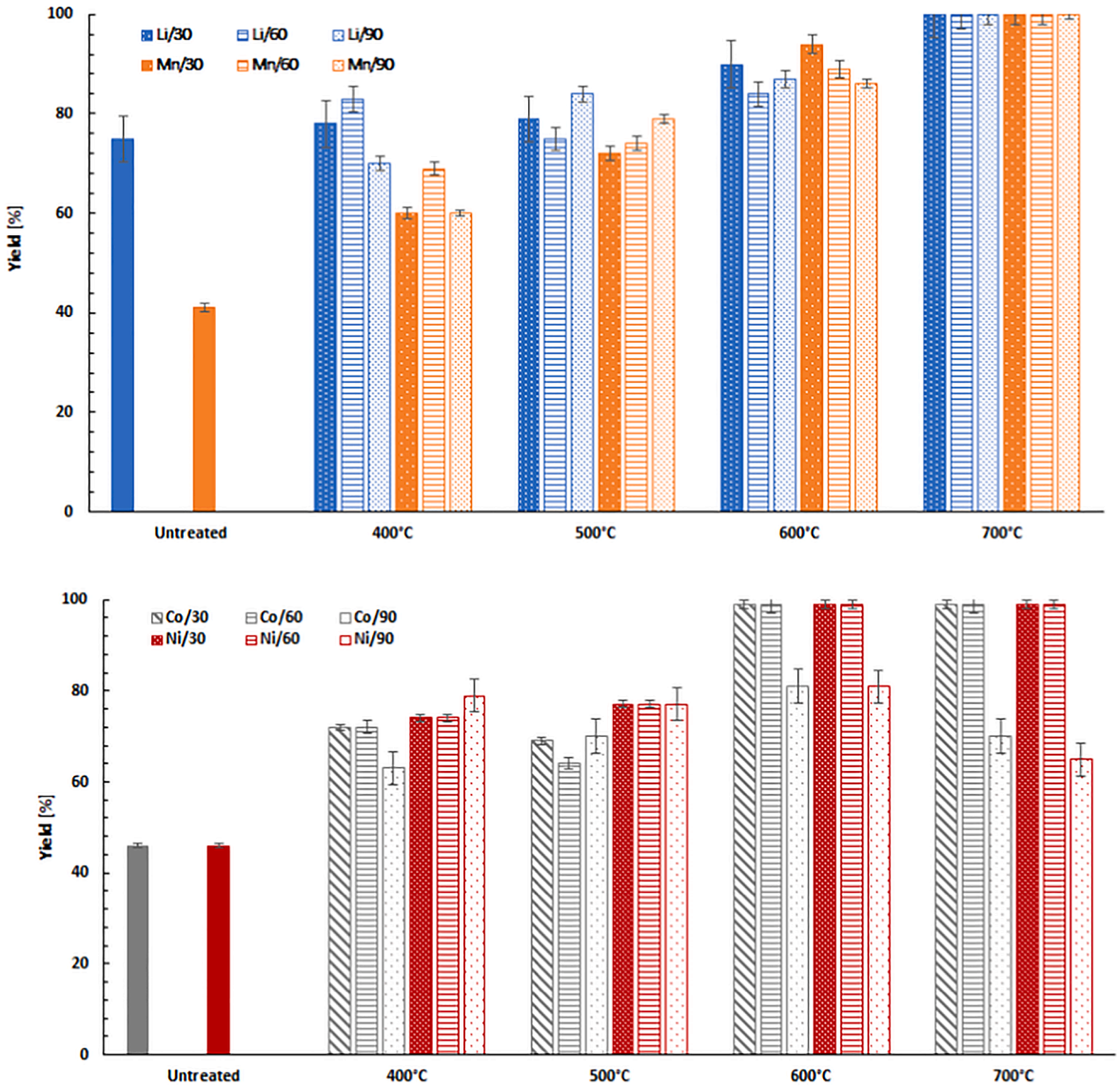

Fig. 5. Leaching yield of Mn (orange bars) and Li (blue bars) from the pyrolyzed samples after different duration (30, 60 and 90 min) of the processing and Leaching yield of Co (brown bars) and Ni (red bars) from the pyrolyzed samples after different duration (30, 60 and 90 min) of the processing. Leaching conditions: 1 h, 25 °C, 2 M H_2SO_4, solid to liquid ratio of 1:50 (g/mL). (For interpretation of the references to colour in this figure legend, the reader is referred to the web version of this article.)

Table 3
Processing temperatures in ascending order of leaching kinetics.

Incineration	Li	700 °C = 400 °C < Untreated < 500 °C = 600 °C
	Mn	700 °C < Untreated = 400 °C = 600 °C < 500 °C
	Co, Ni	700 °C < 600 °C < 400 °C < Untreated < 500 °C
Pyrolysis	Li, Mn, Co, Ni	Untreated < 400 °C < 500 °C < 700 °C < 600 °C

incineration if further hydrometallurgical processing is applied for metal recovery. Faster kinetics and more consistent and controlled leaching products are obtained. Pyrolysis at 700 °C for 30 min are the optimal parameters for the subsequent leaching process. Under these conditions, complete leaching of Li was reached in 2 min. Based on the results, it can be concluded that pyrolysis promotes the formation of lithium carbonate (soluble in water) in larger extend thanincineration. In the present study, final lithium products were not crystalized after the leaching and therefore the amount of lithium carbonate formed during pyrolysis and incineration was not quantitatively determined. However, the comparison of the leaching efficiencies of lithium in Fig. 1 and Fig. 4 clearly confirm the positive influence of pyrolysis.

Under the tested conditions, approximately 5 min are required to fully leach Mn, while 10 min are needed to recover both Co and Ni. To avoid exceeding the melting point of aluminium, using a pyrolysis temperature of 600 °C would be recommended since the metal recovery after such treatment is also sufficient. Also, it has to be considered that pyrolysis is a more environmental-friendly process than incineration for the removal of organic compounds from LiBs, since by-products can be further utilized (Lombardo et al., 2020).

4. Conclusions

It was determined that the products of incineration and pyrolysis at different temperatures differ. The oxygen consumes most of the carbon present in the samples during the incineration. Thus, incineration reduces the feasibility of carbothermic reduction of Co, Mn and Ni oxides into more soluble oxides or even into their metallic forms, which are easier to leach. For pyrolysis instead, the carbothermic reduction is more controlled since the inert atmosphere enhances the reduction

conditions.

Although increasing the incineration temperature does not promote any clear benefit to the leaching yield or kinetics, the temperature does have a positive impact on pyrolyzed samples. The leaching yield is improved when the pyrolysis temperature increases. Leaching yields also increase from untreated samples to pyrolysis at 700 °C and at this temperature, all the Li, Mn, Co and Ni are leached. A gradual improvement in the leaching yield is observed when the temperature of pyrolysis is increased from 400 to 600 °C. For pyrolysis at 700 °C, increasing the time of thermal treatment decreases the leaching yield from 100% in 30 and 60 min, to 70% in 90 min for Co and Ni. Kinetics is also slower when the time is increased.

If all the tested variables are taken into account, namely temperature, time and type of thermal treatment, pyrolysis at 700 °C for 30 min are the best parameters. Under these conditions, full recovery via leaching with sulfuric acid at ambient temperature is reached after 2 min for Li, 5 min for Mn and 10 min for both Co and Ni. Performing pyrolysis before the leaching in a Li-ion battery recycling process is a promising pre-treatment approach, which can not only ease the industrialization of recycling but also the pyrolysis products can be reclaimed.

Declaration of Competing Interest

The authors declare that they have no known competing financial interests or personal relationships that could have appeared to influence the work reported in this paper.

Acknowledgement

This research was supported by the Swedish Energy Agency – Battery fund (Grant No: 40506-1 and 48204-1).

References

Balachandran, S., Forsberg, K., Lemaître, T., Vieceli, N., Lombardo, G., Petranikova, M., 2021. Comparative Study for Selective Lithium Recovery via Chemical Transformations during Incineration and Dynamic Pyrolysis of EV Li-Ion Batteries. Metals 11 (8), 1240. https://doi.org/10.3390/met11081240.

Chagnes, A., Swiatowska, J., 2015. Lithium Process Chemistry. Elsevier.

Huang, Z., Zhu, J., Qiu, R., Ruan, J., Qiu, R., 2019. A cleaner and energy-saving technology of vacuum step-by-step reduction for recovering cobalt and nickel from spent lithium-ion batteries. Journal of Cleaner Production 229, 1148–1157.

Lee, C.K., Rhee, K.-I., 2003. Reductive leaching of cathodic active materials from lithium ion battery wastes. Hydrometallurgy 68 (1-3), 5–10.

Lombardo, G., 2019. Effects of pyrolysis and incineration on the chemical composition of Li-ion batteries and analysis of the by-products. Chalmers University of Technology, Gothenburg.

Lombardo, G., Ebin, B., Foreman, M.R.S.J., Steenari, B.-M., Petranikova, M., 2020. Incineration of EV Lithium-ion batteries as a pretreatment for recycling – determination of the potential formation of hazardous by-products and effects on metal compounds. Journal of Hazardous Materials 393, 122372. https://doi.org/10.1016/j.jhazmat.2020.122372.

Mantuano, D.P., Dorella, G., Elias, R.C.A., Mansur, M.B., 2006. Analysis of a hydrometallurgical route to recover base metals from spent rechargeable batteries by liquid–liquid extraction with Cyanex 272. Journal of Power Sources 159 (2), 1510–1518.

Meshram, P., Pandey, B.D., Mankhand, T.R., 2015. Recovery of valuable metals from cathodic active material of spent lithium ion batteries: Leaching and kinetic aspects. Waste Management 45, 306–313.

Nan, J., Han, D., Zuo, X., 2005. Recovery of metal values from spent lithium-ion batteries with chemical deposition and solvent extraction. Journal of Power Sources 152, 278–284.

Ordoñez, J., Gago, E.J., Girard, A., 2016. Processes and technologies for the recycling and recovery of spent lithium-ion batteries. Renewable and Sustainable Energy Reviews 60, 195–205.

Outotec, 2016. HSC Chemistry 9.

Peng, C., Lahtinen, K., Medina, E., Kauranen, P., Karppinen, M., Kallio, T., Wilson, B.P., Lundström, M., 2020. Role of impurity copper in Li-ion battery recycling to LiCoO2 cathode materials. Journal of Power Sources 450, 227630. https://doi.org/10.1016/j.jpowsour.2019.227630.

Petranikova, M., Miskufova, A., Havlik, T., Forsen, O., Pehkonen, A., 2011. Cobalt recovery from spent portable lithium accumulators after thermal treatment. Acta Metall Slovaca 17, 106–115.

Porvali, A., Chernyaev, A., Shukla, S., Lundström, M., 2020. Lithium ion battery active material dissolution kinetics in Fe(II)/Fe(III) catalyzed Cu-H2SO4 leaching system. Separation and Purification Technology 236, 116305. https://doi.org/10.1016/j.seppur.2019.116305.

Shin, S.M.S., Kim, N.H., Sohn, J.S., Yang, D.H., Kim, Y.H., 2005. Development of metals recovery process from Li-ion battery waste. Hydrometallurgy 79, 172–181.

Sun, L., Qiu, K., 2011. Vacuum pyrolysis and hydrometallurgical process for the recovery of valuable metals from spent lithium-ion batteries. Journal of Hazardous Materials 194, 378–384.

Tang, Y., Xie, H., Zhang, B., Chen, X., Zhao, Z., Qu, J., Xing, P., Yin, H., 2019. Recovery and regeneration of LiCoO2-based spent lithium-ion batteries by a carbothermic reduction vacuum pyrolysis approach: Controlling the recovery of CoO or Co. Waste Management 97, 140–148.

Toro, N., Rodríguez, F., Rojas, A., Robles, P., Ghorbani, Y., 2021. Leaching manganese nodules with iron-reducing agents – A critical review. Minerals Engineering 163, 106748. https://doi.org/10.1016/j.mineng.2020.106748.

Zhang, G., He, Y., Wang, H., Feng, Y.i., Xie, W., Zhu, X., 2019. Application of mechanical crushing combined with pyrolysis-enhanced flotation technology to recover graphite and LiCoO2 from spent lithium-ion batteries. Journal of Cleaner Production 231, 1418–1427.

Zhang, P., Yokoyama, T., Itabashi, O., Suzuki, T.M., Inoue, K., 1998. Hydrometallurgical process for recovery of metal values from spent lithium-ion secondary batteries. Hydrometallurgy 47 (2-3), 259–271.